Article

Tertiary Structure Changes in Albumin upon Surface Adsorption Observed via Fourier Transform Infrared Spectroscopy

Jack R. Smith, Marcus T. Cicerone, and Curtis W. Meuse

Langmuir, **Article ASAP** • DOI: 10.1021/la802955w • Publication Date (Web): 10 March 2009

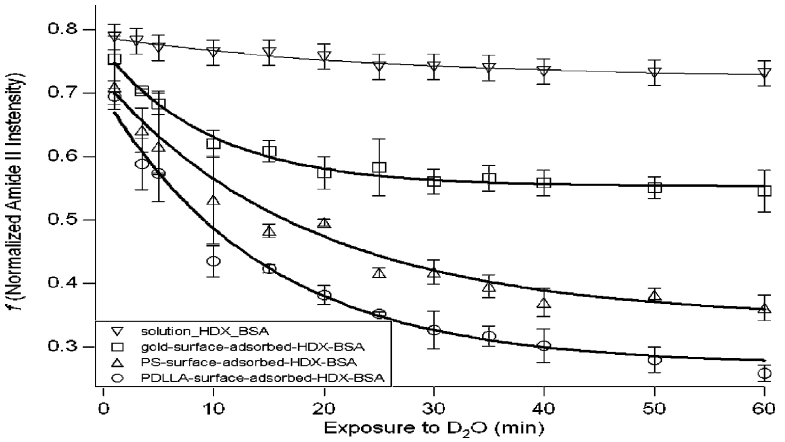

More About This Article

Additional resources and features associated with this article are available within the HTML version:

- Supporting Information
- Access to high resolution figures
- Links to articles and content related to this article
- Copyright permission to reproduce figures and/or text from this article

View the Full Text HTML

Langmuir
Article
pubs.acs.org/Langmuir

Tertiary Structure Changes in Albumin upon Surface Adsorption Observed via Fourier Transform Infrared Spectroscopy

Jack R. Smith,[†] Marcus T. Cicerone,[†] and Curtis W. Meuse*[,‡]

[†]*Polymers Division, Materials Science and Engineering Laboratory, National Institute of Standards and Technology, Gaithersburg, Maryland 20899-8543 and* [‡]*Biochemical Science Division, Chemical Science and Technology Laboratory, National Institute of Standards and Technology, Gaithersburg, Maryland 20899-8313*

Received September 8, 2008. Revised Manuscript Received January 23, 2009

A nondestructive Fourier transform infrared (FTIR) spectroscopy assay, amenable to exploring a wide range of proteins and polymers, is used to measure changes in the tertiary structure of bovine serum albumin (BSA) adsorbed to three surfaces: gold, polystyrene (PS), and poly(D,L-lactic acid) (PDLLA). Tertiary structural analysis is important because typical secondary structural analysis (FTIR and CD) is not always sensitive enough to distinguish between the sometimes subtle protein structural changes caused by adsorption. The polymers are spin-coated onto a gold surface, exposed to protein, and then immersed in a deuterated buffer solution to probe the protein's tertiary structure before the sample is removed from its aqueous environment. Infrared band intensities, related to the exchange of amide hydrogen for deuterium (HDX), as a function of the immersion time in deuterated buffer, are used to determine the extent of amide solvent exposure. Analysis of the results in terms of a single exponential decay shows that enough amides undergo a measurable amount of exchange in 60 min to quantify relative changes in BSA solvent exposure on different surfaces. In addition, substantial fractions undergo HDX at a rate too fast or too slow to be followed with our experimental protocol. The proportions of these quickly and slowly exchanging amide groups also provide information about relative changes in the BSA structure on different surfaces. Adsorption was found to increase the extent of HDX over that observed for BSA in solution, consistent with surface-induced unfolding and a loss of tertiary structure. Changes in HDX were found to be more sensitive to which surface was absorbing the protein than the typical FTIR secondary structural analysis obtained from fitting the amide I band. HDX was greatest for BSA adsorbed to the surface of PDLLA and least in the case of BSA adsorbed to gold, which indicates the greatest and least degree of unfolding, respectively.

Introduction

Both protein-resistant and surface-functionalized biomimetic materials[1−3] have been developed for a variety of biomedical and implant applications. However, these types of materials cannot meet all the needs of tissue scaffold applications (e.g., ability to degrade, mechanical property requirements, etc.). In order to meet these requirements, the protein/surface interactions involved in nonspecific biological response to materials need to be quantitatively understood. Protein/surface interactions are also relevant to pharmaceutical, biosensor, contact lens, and a variety of other technologies.[4−8] In all cases, it is essential to know when surface interactions are severe enough to alter protein structure; simply quantifying the amount of adsorbed protein is insufficient. This is particularly important in materials design for regenerative medicine where surface interactions can inactivate protein segments, such as the RGD tripeptide (arginyl−glycyl−aspartic acid) portion of fibronectin, relevant to the attachment and proliferation of tissue forming cells.[9−13] Recent results[14] have even demonstrated that the distortion of the structure of albumin and fibrinogen upon adsorption to polypropylene can significantly alter the adhesion of platelets.

There are many tools available to study protein adsorption. The most widely applied techniques, using radio or fluorescently labeled proteins, are sensitive and reliable indicators of the amount of adsorbed protein but give little information regarding tertiary structure.[15−19] Atomic force microscopy

*Author to whom correspondence should be addressed. Mailing address: 100 Bureau Dr., Stop 8313, Gaithersburg, MD 20899-8313. Telephone: (301) 975-5311. E-mail: curtis.meuse@nist.gov.

(1) Roberts, C.; Chen, C. S.; Mrksich, M.; Martichonok, V.; Ingber, D. E.; Whitesides, G. M. *J. Am. Chem. Soc.* **1998**, *120*, 6548–6555.
(2) Yeo, W. S.; Yousaf, M. N.; Mrksich, M. *J. Am. Chem. Soc.* **2003**, *125*, 14994–14995.
(3) Orner, B. P.; Derda, R.; Lewis, R. L.; Thomson, J. A.; Kiessling, L. L. *J. Am. Chem. Soc.* **2004**, *126*, 10808–10809.
(4) Kasemo, B. *Surf. Sci.* **2002**, *500*, 656–677.
(5) Texter, J.; Tirell, M. *AIChE J.* **2001**, *47*, 1706–1710.
(6) Gray, J. J. *Curr. Opin. Struct. Biol.* **2004**, *14*, 110–115.
(7) Castner, D. G.; Ratner, B. D. *Surf. Sci.* **2002**, *500*, 28–50.
(8) Magnani, A.; Peluso, G.; Maragarucci, S.; Chittur, K. K. In *Integrated Biomaterials Science*; Kluwer Academic/Plenum: New York, **2002**.
(9) Horbett, T. A. In *Biopolymers at Interfaces*, 2nd ed.; Malmsten, M., Ed.; Marcel Dekker, Inc.; New York, **2003**; pp 393−413.
(10) d'Souza, S. E.; Ginsberg, M. H.; Plow, E. F. *Trends Biochem. Sci.* **1991**, *16*, 246–250.
(11) Ruoslahti, E.; Pierschbacher, M. D. *Cell* **1986**, *44*, 517–518.
(12) Koo, L. Y.; Irvine, D. J.; Mayes, A. M.; Lauffenburger, D. A.; Griffith, L. G. *J. Cell Sci.* **2002**, *115*, 1423–1433.
(13) Shen, M.; Horbett, T. A. *J. Biomed. Mater. Res.* **2001**, *57*, 336–345.
(14) Hylton, D. M.; Shalaby, S. W.; Latour, R. A. *J. Biomed. Mater. Res.* **2005**, *73A*(3), 349–358.
(15) Roach, P.; Farrar, D.; Perry, C. C. *J. Am. Chem. Soc.* **2005**, *127*, 8168–8173.
(16) Slack, S. M.; Horbett, T. A. *J. Colloid Interface Sci.* **1989**, *26*, 1633–1649.
(17) Weber, N.; Bolikal, D.; Bourke, S. L.; Kohn, J. *J. Biomed. Mater. Res.* **2004**, *68A*, 496–503.
(18) Cornelius, R. M.; Wjciechowski, P. W.; Hove, P. T.; Brash, J. L. *J. Colloid Interface Sci.* **1986**, *150*, 121–133.
(19) Tsai, W.-B.; Grunkemeier, J.; Horbett, T. A. *J. Biomed. Mater. Res.* **2003**, *67A*, 1255–1268.

 DOI: 10.1021/la802955w

(AFM) does provide a means to obtain structural information;[20−23] however, obtaining it over the square micrometer scale surface areas relevant to high-throughput materials development is not feasible. More promising are circular dichroism (CD) spectroscopy[14,24−26] and Fourier transform infrared (FTIR) spectroscopy.[15,27,28] These techniques provide surface-averaged results, are nondestructive, can deduce relative conformational changes of solution-suspended and surface-adsorbed proteins, and are not limited by the molecular weight of the sample.[29] Generally, both techniques involve a curve fitting analysis to determine the amounts of several different types of protein secondary structure present in the surface layers of protein and compare these amounts with the amounts of the secondary structures of the same proteins in solution.[14,15,24−29] The problem is that, even under ideal conditions without issues of protein orientation at the surface, the standard error of prediction in cross validation is 5.5% for the α-helix, 6.6% for the β-sheet, and 3.4% for the β-turn.[30] While carefully controlled specific experiments[15] may have smaller errors for reproducibility, these reported standard errors do not provide much confidence in detailed comparisons of protein structures on different surfaces where protein orientation and spectral signal-to-noise issues may play a larger role. Here, we adapt the FTIR spectroscopy approach previously used to measure the structural stability of proteins in solution via amide hydrogen−deuterium exchange (HDX)[31,32] for surface applications.

HDX can be measured by various means including mass spectrometry[33,34] and nuclear magnetic reasonance.[35,36] In this paper, we present a method to obtain this information using FTIR spectroscopy to measure protein amide HDX in monolayers on surfaces. The work complements other studies using FTIR and HDX to characterize the conformation and hydration properties of bovine serum albumin (BSA) films with thicknesses on the order of micrometers[37] and the influence of ligand binding in solution.[32] The nondestructive nature of our method to interrogate the conformation of proteins in contact with planar surfaces suggests it can be used directly before biological response (e.g., cellular attachment, etc.) experiments. While we demonstrate its application in the case of BSA adsorption onto the surface of gold and two polymers, we emphasize that the method is amenable to the exploration of a wide range of proteins and adsorbing materials. In addition, the same FTIR data obtained may provide secondary structural information about the nondeuterated, adsorbed protein.[15] Ultimately, we intend for the combined techniques to provide a comprehensive and quantitative analysis of adsorbed protein structure that is amenable to a high-throughput analysis of protein/polymer interactions. Current experiments include measuring the relative conformations of fibronectin on protein gradient samples as well as on RGD gradient samples. In this way, we hope the technique will become a useful tool in combinatorial biomaterials development.

Materials and Methods[38]

Preparation of Buffers. Stock solutions of all hydrogen (all-H) and deuterated 0.01 M sodium phosphate buffer (Sigma) at pH 7.8 (pD = pH + 0.4[39,40]) were prepared using either deionized H_2O or D_2O (Cambridge Isotope Laboratories, Inc.). The all-H sodium phosphate buffer will hereafter be referred to as "HSPB", while the deuterated version will hereafter be referred to as "DSPB."

Preparation and Routine Characterization of Sample Surfaces. Silicon wafers, precoated with 100.0 nm of gold by the manufacturer (Platypus Technologies, Madison, WI), were sectioned into 10 2 cm × 2 cm pieces. These pieces will hereafter be referred to as "wafer sections", and "uncoated wafer section" will refer to a gold-covered silicon wafer section that has not been spin-coated with polymer. The air−water contact angle (θ) of an uncoated wafer section was measured using a G2 contact angle measuring system (Krüss, Matthews, NC), and θ was (86 ± 1)° over five trials.

Both polystyrene (PS) and poly(D,L-lactic acid) (PDLLA) (Polysciences, Warrington, PA) were received in pellet form. For PS, the relative molecular mass was 250 000 g/mol. PDLLA is a random copolymer whose repeat units appear in Figure 1A. The relative molecular mass of the PDLLA was between 330 000 and 600 000 g/mol. One mg/mL solutions of polymer in HPLC-grade methylene chloride solution (Aldrich) were prepared for spin-coating wafer sections. Two mL of the solution was then dropped onto the gold-coated side of a wafer section spinning at 2500 rpm. Both the wafer revolution rate and the polymer concentration in the methylene chloride solution were optimized to produce thin, homogeneous films. Slower spinning rates and higher polymer concentrations led to thicker polymer layers that were too optically heterogeneous for quantitative analysis. Six of the wafer sections were spin-coated with a (5−10) nm layer of polymer, three with polystyrene (PS), and three with PDLLA. Goniometry measurements (as described above) gave contact angles of (78 ± 2)° and (110 ± 1)° for PDLLA and PS, respectively.

The thicknesses of the spin-coated polymer layers as well as the adsorbed protein layers were measured using a model 44

(20) Siedlecki, C. A.; Marcant, R. E. *Biomaterials* **1998**, *19*, 441–454.
(21) Haggerty, L.; Watson, B. A.; Barteau, M. A.; Lenhoff, A. M. *J. Vac. Sci. Technol., B* **1991**, *9*(2), 1219–1222.
(22) Eppell, S. J.; Simmons, S. R.; Albrecht, R. M.; Marchant, R. E. *Biophysics* **1995**, *68*, 671–680.
(23) Feng, L.; Andrade, J. D. *J. Biomed. Mater. Res.* **1993**, *27*(2), 177–182.
(24) McMillin, C. R. *J. Colloid Interface Sci.* **1974**, *48*, 345–349.
(25) Herrick, S.; Blanc-Brude, O.; Gray, A.; Laurent, G. *Int. J. Biochem. Cell Biol.* **1999**, *31*, 741–746.
(26) Bondelle, S. E.; Ostresh, J. M.; Houghten, R. A.; Perez-Pay, E. *Biophysics* **1995**, *68*, 351–359.
(27) Noinville, S.; Bruston, F.; Amri, C. E.; Baron, D.; Nicolas, P. *Biophys. J.* **2003**, *85*, 1196–1206.
(28) Xie, J.; Riley, C.; Kumar, M.; Chittur, K. *Biomaterials* **2002**, *23*(17), 3609–3616.
(29) Jackson, M.; Mantsch, H. H. *Crit. Rev. Biochem. Mol. Biol.* **1995**, *30*, 95–120.
(30) Goormaghtigh, E.; Ruysschaert, J. M.; Raussens, V. *Biophys. J.* **2006**, *90*, 2946–2957.
(31) Vrettos, J. S.; Meuse, C. W. *Anal. Biochem.* Submitted for publication.
(32) Celej, M. S.; Montich, G. G.; Fidelio, G. D. *Protein Sci.* **2003**, *12*, 1496–1506.
(33) Larsericsdotter, H.; Oscarsson, S.; Buijis, J. *J. Colloid Interface Sci.* **2004**, *276*, 261–268.
(34) Sokol, J. M.; Holmes, B. W.; O'Connell, J. P.; Fernandez, E. J. *J. Chromatogr., A* **2003**, *1007*(1−2), 55–66.
(35) LiWang, A. C.; Bax, A. *J. Am. Chem. Soc.* **1996**, *118*, 12864–12865.
(36) Englander, S. W.; Sosnick, T; Englander, R.; Mayne, J. J. *Curr. Opin. Struct. Biol.* **1996**, *6*, 18–23.
(37) Grdadolnik, J.; Marechal, Y. *Appl. Spectrosc.* **2005**, *59*, 1347–1356.

(38) Certain commercial equipment, instruments, or materials are identified in this paper in order to specify the experimental procedure adequately. Such identification is not intended to imply recommendation or endorsement by the National Institute of Standards and Technology, nor is it intended to imply that the materials or equipment identified are necessarily the best available for the purpose. The "SD of the mean" is the same as the "combined standard uncertainty of the mean" for the purposes of this work.

(39) Whisenhunt, D. W.Jr; Neu, M. P.; Hou, Z.; Xu, J.; Hoffman, D. C.; Raymond, K. N. *Inorg. Chem.* **1996**, *35*, 4128–4136.
(40) Bates, G. R. *Determination of pH: Theory and Practice*; Wiley: New York, **1964**.

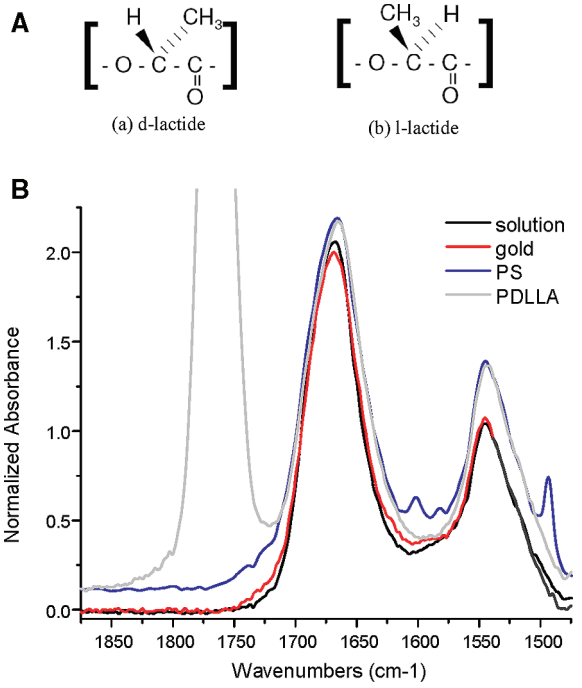

Figure 1. (A) PDLLA is a random copolymer with (a) D- and (b) L-lactide repeat units. (B) Comparison of the $t = 0$ spectra for different BSA samples scaled to the same amide I intensity and then offset for clarity. Black, multilayer BSA sample from solution; red, BSA adsorbed to gold surface; blue, BSA adsorbed to PS; and light gray, BSA adsorbed to PDLLA.

spectroscopic ellipsometer (J. A. Woollam, Lincoln, NE) using a method described elsewhere.[41]

Fourier Transform Infrared Spectroscopy. Infrared spectra were obtained using an Equinox 55 Fourier transform infrared spectrometer (Bruker, Billerica, MA) equipped with a KBr beam splitter and a liquid-nitrogen-cooled mercury cadmium telluride (MCT) detector. The sample chamber was purged with dry air from a purge gas generator (Whatman, Haverhill, MA). Samples were placed on a VeeMax reflection accessory (Pike Technologies, Madison, WI) such that the p-polarized (ZnSe wire grid polarizer, Harrick Scientific, Ossining, NY) IR beam had an angle of incidence of 75°. After each sample was placed on the chamber, the dry air purge was allowed to remove ambient water vapor from the chamber for 10 min. Spectra were then collected at five randomly chosen positions on the sample surface and averaged. The spectra were collected and averaged from different sample positions to account for any lateral heterogeneities in the adsorbed protein reflectivity. A typical spectral measurement consisted of 100 scans at 2 cm^{-1} resolution. Absorbance spectra were obtained relative to an analogous measurement on a reference (protein-free, gold-coated) wafer and calculated as $-\log_{10}$ (sample/reference).

The influences of water vapor on the spectrum were eliminated via spectral subtraction as follows: A blank wafer sample was placed on the sample stage, and scans were taken both before and after 30 min of dry air purge. Water vapor absorbance spectra were calculated as the negative logarithm of the ratio of these scans. Water vapor absorbance spectra were then subtracted from the absorbance spectra of each sample in order to eliminate the narrow water vapor bands occurring between 1900 and 1300 cm^{-1}.

HDX Measurements. Here, we adapt a protocol that provides adsorbed protein monolayers from concentrated protein solutions, which, in general, yield multiple layers of proteins.[42] Immersing a deuteron-free (all-H) protein in a D_2O-based buffer at $t = 0$ will cause amide groups in the protein to exchange their hydrogen atoms for deuterons. The proportion of amide nitrogen atoms in the protein bonded to deuterons compared to the total number of amides (hereafter referred to as "the extent of HDX") will then increase until full deuteration is reached. If the structure of the protein is unfolded, then it will exhibit a greater extent of HDX at any time, t, than it would in its native conformation because of the increased exposure of the amide groups to deuterated solvent.[36,43,44] Samples of BSA with HDX properties reflecting the surface-adsorbed state were prepared and measured as described below. The procedure for preparing the adsorbed protein layer was identical for both polymer-coated and uncoated wafer sections. It was repeated three times each for BSA adsorbed to gold, BSA adsorbed to PS, and BSA adsorbed to PDLLA.

Lyophilized, all-H BSA (Sigma, CAS #9048-46-8, fatty acid content < 0.02%) was added to HSPB so that the final concentration of protein was 20 mg/mL and the resulting deuteron-free protein solution was placed in a polystyrene Petri dish. Wafer sections were then kept in the solution for 2 h in order to allow a layer of all-H BSA to form on its surface. Subsequently, the wafer section was removed but not dried and placed in a second polystyrene Petri dish which was filled with protein-free HSPB. The purpose of this latter step was to remove all but the irreversibly adsorbed protein from the surface of the wafer sample. After 15 min, the $t = 0$ wafer sections were removed and dried under nitrogen for 1−2 s, and then FTIR spectra were obtained. Up to this point, the surface-adsorbed BSA layer had not been exposed to deuterons. Finally, HDX was initiated by placing the wafer sections in DSPB. The extent of HDX in the layer of BSA adsorbed to the wafer section surface was monitored 12 times at specified exposure intervals (1.5, 3, 5, 10, 15, 20, 25, 30, 35, 40, 50, and 60 min). The wafer section was removed from the DSPB and dried under nitrogen gas to arrest HDX, FTIR spectra were acquired, and the sample was subsequently returned to the DSPB. In the discussion that follows, each such sample will be referred to as "X-surface-adsorbed-HDX-BSA" where X = surface type (i.e., gold, PS, or PDLLA).

Samples of BSA with HDX properties reflecting the native or solution conformation were prepared and measured as follows: A polystyrene vial was filled with a 30 mL aliquot of protein-free DSPB. Subsequently, solution-state HDX was initiated by adding lyophilized, all-H BSA (Sigma, CAS #9048-46-8, fatty acid content < 0.02%) to the vial until the final concentration was 20 mg/mL. The extent of HDX in solution-suspended BSA was monitored at 12 specified exposure times (1, 3, 5, 10, 15, 20, 25, 30, 35, 40, 50, and 60 min), dried (in 1−2 s) under nitrogen gas to arrest HDX. A 0.5 mL aliquot of the protein solution was removed from the vial and then pipetted onto an uncoated wafer section similarly dried. This created a 25.0−35.0 nm multilayer of dried protein on each of the 12 wafer sections. FTIR spectra were then collected for each wafer section. A deuteron-free sample was obtained by drying 1 mL of SPB containing 20 mg/mL BSA. Finally, it should be noted that while the wafer drying time was short compared to the specified HDX exposure times (< 3%), and the protein layers were very thin, it is possible that some further HDX occurred before evaporation was complete.

The solution samples described in the previous paragraph are layers of dried solution several times thicker than that of a surface-adsorbed monolayer. The contribution of the surface-adsorbed monolayer to the spectra taken on these samples is

(41) Meuse, C. W.; Kreuger, S.; Majkrzak, C.; Dura, J.; Fu, J.; Conner, J.; Plant, A. L. *Biophys. J.* **1998**, *74*, 1388–1398.

(42) Smith, J. R.; Cicerone, M. T.; Meuse, C. W. *J. Colloid Interface Sci.* Submitted for publication.

(43) Huyghues-Despointes, B. M. P.; Pace, C. N.; Englander, S. W.; Scholtz, J. M. *Methods Mol. Biol.* **2001**, *168*, 69–92.

(44) Huyghues-Despointes, B. M. P.; Scholtz, J. M.; Pace, C. N. *Nat. Struct. Biol.* **1999**, *6*, 910–912.

expected to be small. We expect amide HDX in these samples to reflect the conformation BSA adopts while suspended in DSPB. In the discussion that follows, these samples will be referred to as "solution-HDX-BSA."

Finally, it should be noted that other factors, such as pH, moieties other than amides exchanging or absorbing near 1550 cm^{-1}, and surface microheterogeneity, could alter the correlation between the degree of HDX and the absolute degree of protein unfolding. Therefore, it is important to run experiments under as close to identical conditions as possible to derive a robust *relative* measure using HDX.

Data Analysis. We track HDX via the largest change in the IR spectrum with amide deuteration, that is, the decrease of amide II band intensity. This band is assigned to the N−X in-plane bending mode of the amide linkages and shifts from around 1550 cm^{-1} for X = H to around 1450 cm^{-1} for X = D. We quantify the fraction of amide groups in the protein that have retained their hydrogen atoms at any given exposure time, t, to DSPB as[42]

$$f(t) = \frac{I_{\mathrm{AmideII}}(t)}{I_{\mathrm{AmideII}}(0)} \quad (1)$$

where $I_{\mathrm{AmideII}}(t)$ is the amide II band intensity at t and $I_{\mathrm{AmideII}}(0)$ is the intensity of amide II in the absence of deuteration. Note that eq 1 is normalized with respect to the nondeuterated amide II intensity and that f *decreases* with the degree of amide exposure to solvent or the degree to which the protein structure is unfolded. For clarity, we define "the extent of HDX" at t as

$$\text{extent of HDX} = 1 - f(t) \quad (2)$$

In the discussion that follows, the extent of HDX calculated via eq 2 is expressed in terms of a percentage. Note that the extent of HDX at 60 min reflects exchange for only a subset of the hundreds of amide groups in the protein.

The complete process of exchange can be modeled via a multiexponential decay[32] where each exponential represents a different rate-limiting mechanism. Because our experiment is finite, however, we divide the HDX measured into two constant components and a single exponential. The constant components represent amides with exchange rates too slow or too fast to be measured in our 60 min experiment, while those with intermediate exchange rates are represented by the exponential component. A nonlinear least-squares (Levenberg−Marquardt) fit of our data to an exponential decay

$$f_{\mathrm{decay}}(t) = f_{60} + a\,\mathrm{e}^{-kt} \quad (3)$$

allows us to determine the relative contribution of each component from the fitting constants (a, k, and f_{60}). f_{60} is the proportion of amide groups that do not undergo isotope exchange to an appreciable extent in 60 min. This number exhibits a counter-correlation to the extent of HDX (eq 2) and should decrease with unfolding. The exponentially decaying component ($a\,\mathrm{e}^{-kt}$) accounts for amide groups that are shielded from solvent by the protein structure but undergo HDX at an average rate (k) that is measurable in this experiment. We expect the fraction of amide groups represented by this component, that is, a, to increase as surface interactions unfold the protein. The rate constant, k, is useful for comparing conformations of proteins that reach the same extent of HDX (or f_{60} value) within the experiment. In this case, k would quantify differences in the mechanism of the HDX process. We refer to the proportion of amide groups whose exchange occurs too quickly to be measured as f_0. This component is included because initial attempts to use eq 3 to fit f over the entire range in exposure time, that is, t from 0 to 60 min, failed. The fit results dramatically improved when the nondeuterated or t = 0 point was eliminated from the analysis, demonstrating that a sizable amount of exchange had gone to completion prior to the first exchange measurement (i.e., t = 1.5 min). Equation 3 was then used to fit the data from t = 1.5 to 60 min exposure, and f_0 was given as the difference between the value of eq 3 extrapolated to t = 0 and the actual value given by eq 1:

$$f_0 = f(0) - f_{\mathrm{decay}}(0) = \frac{I_{\mathrm{AmideII}}(0)}{I_{\mathrm{AmideII}}(0)} - f_{\mathrm{decay}}(0) = 1 - (a + f_{60}) \quad (4)$$

Results

In Figure 1B, the measurement at t = 0 exposure to deuterated solution provides the data to compare the amide I band from each of our HDX experiments. The center of the amide I bands lie between 1669 cm^{-1} for the solution-HDX-BSA sample and 1667 cm^{-1} for the PDLLA-surface-adsorbed-HDX-BSA. The amide I full-width at half-maximum (fwhm) changes from 38 cm^{-1} for the solution-HDX-BSA sample to 45 cm^{-1} for the PDLLA-surface-adsorbed-HDX-BSA and the PS-surface-adsorbed-HDX-BSA. Since the selection rules of external reflection FTIR allow only bands with components perpendicular to the gold surface to be detected, proteins that orient to different extents upon adsorption cannot be directly compared.[15] When we measure the ratios of the amide II to amide I band intensities, we get 0.51, 0.53, 0.61, and 0.61, respectively, for the solution-HDX-BSA sample, the gold-surface-adsorbed-HDX-BSA, the PS-surface-adsorbed-HDX-BSA, and the PDLLA-surface-adsorbed-HDX-BSA. If we assume that the multilayered solution-HDX-BSA sample is isotropic, then these ratios can be used to determine the orientations of the amide I modes in the samples with respect to the supporting gold surface to be 54.7°, 54°, 52°, and 52°.[15,45] All orientations are reported with an error of ±0.7° over three samples.

Previous work[15] suggests that samples with similar protein orientations, as measured by external reflection FTIR, can be compared using amide I curve fitting analysis for protein secondary structure determination. Although it is unclear how large of orientation differences matter or how to convert orientation differences into secondary structural differences, we chose to undertake secondary structural analysis because we could at least compare the two pairs of samples that had the same orientations as each other within experimental error. Our fit for the solution-HDX-BSA sample using the central wavelengths of 1681, 1656, and 1636 cm^{-1} for β-turns, α-helix, and β-sheet, respectively, reveals 55% turns, 45% helix, and 0% sheet. Our fit for the gold-surface-adsorbed-HDX-BSA reveals 53% turns, 47% helix, and 0% sheet. Our fit for the PS-surface-adsorbed-HDX-BSA reveals 42% turns, 58% helix, and 0% sheet. Our fit for the PDLLA-surface-adsorbed-HDX-BSA reveals 41% turns, 59% helix, and 0% sheet. Once again, we see that the solution and gold have similar results and the PS and PDLLA surfaces have similar results.

(45) Meuse, C. W.; Yang, X.; Yang, D.; Hsu, S. L. *Macromolecules* **1992**, *25*, 925–932.

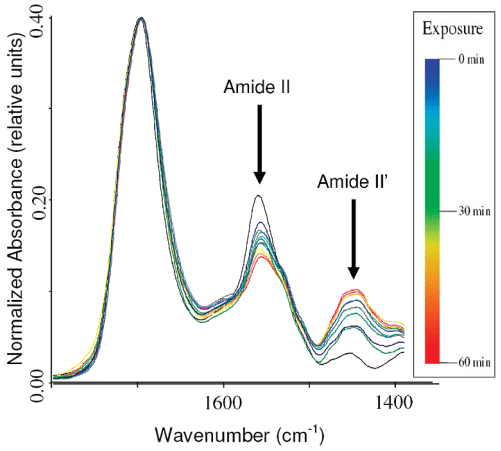

Figure 2. Changes in the amide spectra of BSA in DSPB (solution-HDX-BSA) over the course of 1 h. The spectra are color-coded by exposure time according to the key (inset) and are the average of three experimental trials.

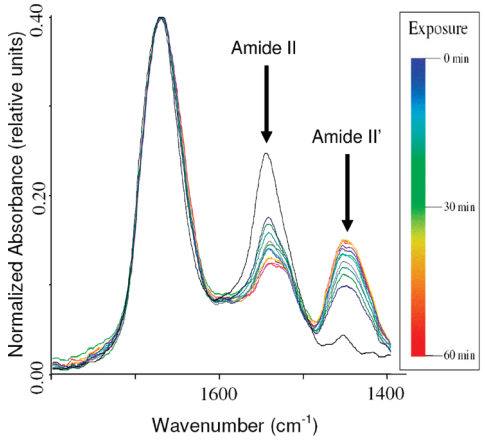

Figure 3. Changes in the amide spectra of a monolayer of BSA adsorbed to the surface of gold and subsequently exposed to DSPB over the course of 1 h. The spectra are color-coded by exposure time according to the key (inset) and are the average of three experimental trials.

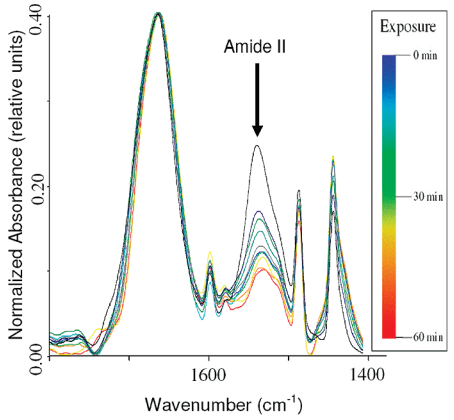

Figure 4. Changes in the amide spectra of a monolayer of BSA adsorbed to the surface of PS and subsequently exposed to DSPB over the course of 1 h. The spectra are color-coded by exposure time according to the key (inset) and are the average of three experimental trials.

Since these values did not look like previous secondary structural analysis for BSA on surfaces,[15] we allowed the center wavelengths to vary. Varying the center wavelengths of our secondary structural analysis of the amide I band shape also did not reveal secondary structures consistent with those in ref 15; however, they did reveal secondary structural percentages similar to those in ref 46. Our fit for the solution-HDX-BSA sample for β-turns, α-helix, and β-sheet, respectively, reveals 28% turns, 63% helix, and 9% sheet. Our fit for the gold-surface-adsorbed-HDX-BSA reveals 43% turns, 57% helix, and 0% sheet. Our fit for the PS-surface-adsorbed-HDX-BSA reveals 30% turns, 49% helix, and 21% sheet. Our fit for the PDLLA-surface-adsorbed-HDX-BSA reveals 43% turns, 43% helix, and 14% sheet.

At first glance, these results to not have many trends. While the decreasing progression of the α-helix content from solution > gold > PS > PDLLA might be taken as an indication of protein unfolding upon adsorption, allowances for the standard error of prediction in cross-validation of 5.5% for the α-helix, 6.6% for the β-sheet, and 3.4% for the β-turn[30] makes it difficult to separate these BSA samples from one another. Even using our average error for the fit of each secondary structure type percentage, $\pm$4%, completely separating the structures of these samples and observing coherent trends proves difficult. Together, the results for the overall band and secondary structural analysis show that the BSA films fall into two groups: the samples from solution and on the gold surface are similar, and the two samples on the polymer surfaces are similar. To further characterize and separate these groups, we utilize HDX tertiary structural analysis to more clearly determine and validate the magnitudes of structural changes upon adsorption.

The FTIR spectra of solution-HDX-BSA appear in Figure 2 as a function of DSPB exposure. These data were acquired on BSA films whose thicknesses ranged from 22.0 to 36.0 nm. One can easily identify the amide I ($\approx$1650 cm^{-1}), amide II ($\approx$1550 cm^{-1}), and amide II′ ($\approx$1450 cm^{-1}) peaks. The amide II and II′ peak intensities decrease and increase, respectively, with increased exposure to deuterated solvent. This is an indication of increased deuteration of amide groups with *t*.

Figure 3 shows an analogous set of FTIR spectra for the gold-surface-adsorbed-HDX-BSA. For this set of BSA films, thicknesses ranged from 3.2 to 7.4 nm, indicating monolayers of protein. Again, the amide II band ($\approx$1550 cm^{-1}) intensity decreases with increasing exposure time, indicating deuteration of amide groups. As we will show below, this occurs to a greater extent than that observed for the solution-HDX-BSA films (Figure 2).

Figures 4 and 5 show the corresponding FTIR spectra for PS-surface-adsorbed-HDX-BSA and PDLLA-surface-adsorbed-HDX-BSA, respectively. The thickness of the protein films adsorbed to the surface of the polymers and gold was identical to within the SD of the mean over five measurements ($\pm$3.0 nm) and ranged from 3.0 to 6.9 nm, indicating a monolayer. Both series of spectra exhibit the protein amide I and II bands as well as polymer peaks. The latter can be easily identified by examining the spectra of the pure polymers (Figure 6 for PS and Figure 7 for PDLLA). In both cases, a polymer peak obstructs the amide II′ peak around 1450 cm^{-1}, but the amide II band used to quantify HDX is unobstructed. The intensity of the amide II band shows the characteristic decrease with intensity with increasing exposure to DSPB, indicating an increase in deuteration of amide groups. As we will show below, this change occurs to a greater extent for

(46) Sjoholm, I; Ljungstedt, I. *J. Biol. Chem.* **1973**, *248*, 8434–8441.

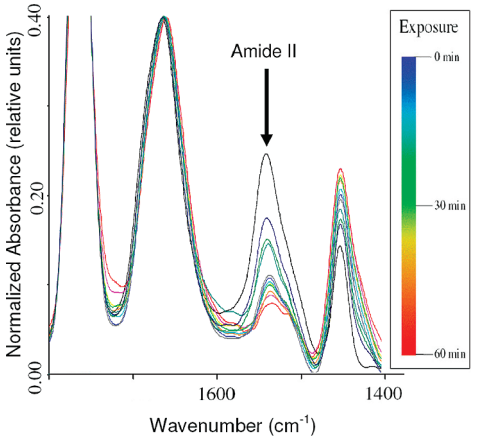

Figure 5. Changes in the amide spectra of a monolayer of BSA adsorbed to the surface of PDLLA and subsequently exposed to DSPB over the course of 1 h. The spectra are color-coded by exposure time according to the key (inset) and are the average of three experimental trials.

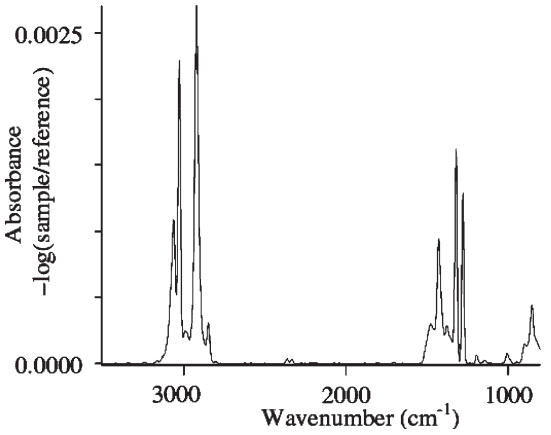

Figure 6. p-Polarized FTIR spectrum of a thin PS film. Sample thickness was approximately (10.2 ± 3.0) nm.

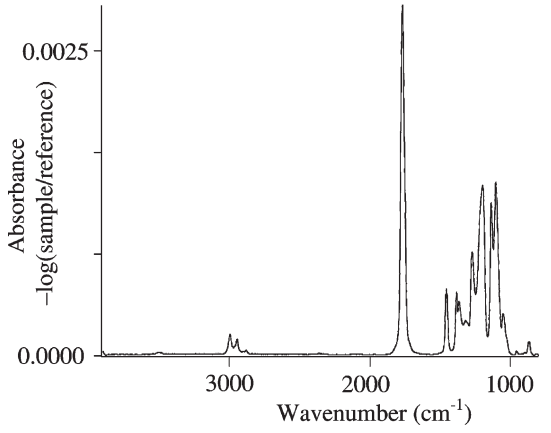

Figure 7. p-Polarized FTIR spectrum of a thin PDLLA film. Sample thickness was approximately (9.7 ± 2.6) nm.

BSA adsorbed to either polymer than for BSA in solution or adsorbed to gold.

Figure 8 shows the change in f with deuteration time. f is calculated via the amide peak intensities from spectra from Figures 2−5 and eq 1 and decreases with increasing levels of deuteration. Peak intensity was quantified as the integrated

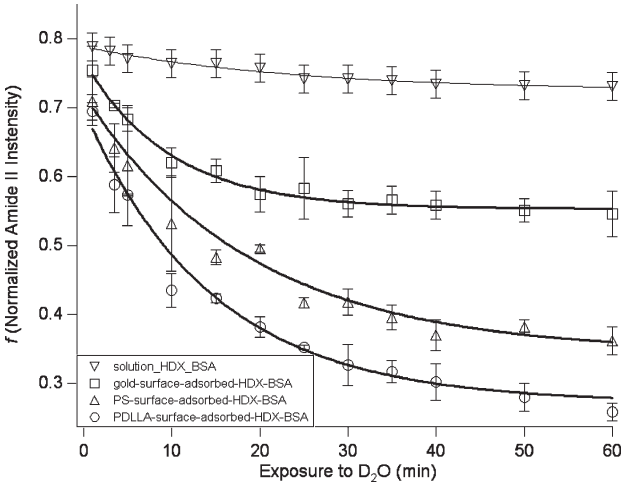

Figure 8. Changes in f for the kinetic experiments as a function of exposure to DSPB. Data points represent the average of five separate spectroscopic measurements. The lines give the results of a nonlinear least-squares (Levenberg−Marquardt) fit to the general exponential decay function (eq 3) [where f is defined in eq 1, t = time (min), and a, k, and f_{60} are the fit coefficients]. The coefficients from the least-squares fit appear in Table 2. Uncertainty bars reflect the SD of the mean of three experimental trials.

intensity of the spectra between 1650 and 1660 cm^{-1} for amide I, and 1540 and 1550 cm^{-1} for amide II.[41] Uncertainty bars in the figure represent the SD of the mean in f over three separate experimental trials. For each of the four types of BSA sample, that is, solution-HDX-BSA and the three surface-adsorbed films, the greatest change in f occurs within the first 20 min of exposure. For both solution-HDX-BSA and gold-surface-adsorbed-HDX-BSA, the change in f after the first 10 min of exposure is small. On the other hand, f for both PS-surface-adsorbed-HDX-BSA and PDLLA-surface-adsorbed-HDX-BSA continues to decrease throughout the entire 60 min experiment.

Discussion

We track HDX via the largest change in the IR spectrum with amide deuteration, that is, the decrease of amide II band intensity. This band is assigned to the N−X in-plane bending mode of the amide linkages and shifts from around 1550 cm^{-1} for X = H to around 1450 cm^{-1} for X = D. The deuterated amide II band at 1450 cm^{-1} is commonly referred to as the "amide II′." The amide II′ band is not used to track HDX, since it is obstructed by peaks from both PS and PDLLA. HDX also results in measurable changes in the amide I band position (occurring around 1650 cm^{-1}) which have been used to quantify amide deuteration.[32] However, our attempts to use this band were less successful, presumably because its shift is small (≤10 cm^{-1}) and the shape of the amide I band exhibits features that reflect aspects of protein secondary structure which may be convoluted with HDX.[15] Therefore, we restrict our quantitative analysis to the amide II band.

A first-order comparison of the HDX behavior for BSA in solution and adsorbed to the gold and polymer surfaces can be obtained by examining the extent of HDX after 60 min exposure to DSPB [calculated via eq 2 and listed in Table 1]. Note that the extent of HDX is quantitatively different for BSA films adsorbed to each surface, even for the BSA films adsorbed to the surfaces of the two polymers. Further, the extent of HDX is greater in every surface-adsorbed case than it is for the solution case. This supports the suggestion that

 DOI: 10.1021/la802955w

Table 1. Average Extent of HDX, as Calculated via eq 2, after 60 min Exposure to DSPB for BSA in Solution and Adsorbed to the Surfaces of Gold, PS, and PDLLA[a]

sample	extent of HDX at 60 min exposure (%)
solution-HDX-BSA	26.8 ± 5.0
gold-surface-adsorbed-HDX-BSA	45.4 ± 3.3
PS-surface-adsorbed-HDX-BSA	63.8 ± 2.0
PDLLA-surface-adsorbed-HDX-BSA	74.1 ± 1.3

[a] Data are averaged over three separate experiments, and the error bars reflect the SD of the mean.

structural changes of the protein upon surface adsorption increase the degree of amide exposure to solvent.

The difference between HDX of surface-adsorbed BSA and BSA in solution is explored more quantitatively by fitting the data to a generalized exponential decay. The data and fits appear in Figure 8, and the fit coefficients are summarized in Table 2. These fits demonstrate that a single exponential decay provides a reasonably good description of the portion of the HDX process described in Figure 8 for surface-adsorbed BSA. k for solution-HDX-BSA, however, is nearly within error of zero. This is because the majority of amide groups (i.e., $f_{60} \approx 0.72$) in that sample do not exchange in 60 min and the monotonic decrease in f in these data (Figure 8) is too small to be fit to an exponential. Indeed, the exponential component in eq 3 accounts for a relatively small fraction of the amide groups in this sample (i.e., $a \approx 0.06$). a is between 2.8 and 8.8 times greater for surface-adsorbed BSA, indicating that a greater fraction of surface-adsorbed amides undergo HDX during the experiment.

Larger a values for surface-absorbed BSA confirms our expectation that the exponential component in eq 3 represents amide groups that are sensitive to surface-induced conformational changes (i.e., those that are buried in the interior of the protein when it is in its native conformation). Further, a shows a counter-trend to f_{60} and is directly related to the extent of HDX (Table 1) from solution-HDX-BSA, gold-surface-adsorbed-HDX-BSA, PS-surface-adsorbed-HDX-BSA to PDLLA-surface-adsorbed-HDX-BSA. This is despite the fact that f_{60} and a are two independent fit parameters and is consistent with the idea that surface-induced unfolding of the tertiary structure of the protein causes an increased exposure of its amide groups. The fraction of amide groups undergoing HDX too quickly to be measured by this experiment (f_0) also increases according to this trend. This means that the proportion of amide groups fully exposed to DSPB increases from solution-HDX-BSA, gold-surface-adsorbed-HDX-BSA, PS-surface-adsorbed-HDX-BSA to PDLLA-surface-adsorbed-HDX-BSA. These are all indications that surface interactions unfold the protein as expected. Finally, comparisons of these results and their errors in Tables 1 and 2 show that HDX tertiary structural analysis clearly separates the samples from one another in terms of the reported errors.

Many of the results presented here are consistent with published reports regarding protein conformation and its response to hydrophobic surfaces. The relatively small extent of HDX for solution-HDX-BSA (Table 1) confirms the expectation that the globular, native conformation of albumin is effective at shielding its interior amide linkages from solvent.[47] We see that interacting with the three surfaces in this experiment results in a more "open" BSA structure, as observed through an increase in amide HDX (Table 1). This agrees with the bulk of the literature showing that BSA unfolds as it sticks to hydrophobic surfaces.[6,14,47−50] The same literature reports suggest that it is not unreasonable for us to see robust quantitative differences in the HDX profiles of each surface-adsorbed film given the substantial range in air−water contact angle ($\theta = 76-110°$). Finally, that BSA unfolds to a greater extent upon adsorption to PS than to gold follows the traditional argument that the denaturing of the protein should increase with surface hydrophobicity.[6,47−50]

Our result showing BSA unfolding is greatest upon adsorption to PDLLA; however, it cannot be explained with empirical relationships between protein conformation and macroscopic surface hydrophobicity. In fact, since the PDLLA surface has the lowest contact angle, such considerations lead us to expect the opposite of what we see.[14] It should be noted that several features of the results including the center wavelength, the percentage of α-helix, as well as the HDX kinetic parameters do not follow the exact order of surface hydrophobicity. This suggests that the result is not an artifact related only to our HDX protocol.

In order to further address the PDLLA result, a more detailed examination of the various factors affecting protein adsorption is warranted. The force between proteins and surfaces is thought to be a convolution of several repulsive (e.g., counterion double layer, steric, hydration) and attractive (e.g., van der Waals, hydrophobic, H-bonding) components.[51−54] Its net magnitude and direction depend not just on surface and protein chemistry but also on factors specific to a particular experimental configuration (e.g., molecule type, fatty acid content, pH).[55−59] The simplest explanation would be that there is a specific attractive interaction such as H-bonding between the PDLLA and the BSA.

Force measurements relevant to our experimental conditions were obtained by Rixman et al.[60] for the interaction of human serum albumin (HSA) with self-assembled monolayer (SAM) surfaces of varying hydrophobicity. While their high-resolution force spectroscopy (HRFS) results show the expected correlation of adhesive force magnitude with air−water contact angle, they also demonstrate energy dissipating mechanisms even in the least hydrophobic case ($\theta \approx 44°$). This implies that the adhesive force between HSA and a surface more hydrophilic than PDLLA is strong enough to alter HSA structure. Rixman et al., however, measured no differences in adhesive force on SAMs with contact angles in the range we explored with our surfaces (i.e., $\theta = 70-110°$). This is despite their measuring a 3-fold difference in adhesive force for the most (~44°) and least hydrophilic SAMs (~110°). In contrast, our HDX profiles (Figure 8) distinguish BSA structures on

(47) Curry, S. *Vox Sang*. **2002**, *83*(Suppl. 1), 315–319.
(48) Wertz, C. F.; Santore, M. M. *Langmuir* **1999**, *15*, 8884–8894.
(49) Wertz, C. F.; Santore, M. M. *Langmuir* **2001**, *17*, 3006–3016.
(50) Lensun, L.; Smith, T. A.; Gee, M. L. *Langmuir* **2002**, *18*, 9924–9931.
(51) Leckband, D. C. *Annu. Rev. Biophys. Biomol. Struct*. **2000**, *29*, 1–26.
(52) Halperin, A.; Leckband, D. C. *C. R. Acad. Sci., Ser. IV: Phys. Astrophys*. **2000**, *IV*, 1171–1178.
(53) Vanderah, D. J.; La, H.; Naff, J.; Silin, V.; Rubinson, K. A. *J. Am. Chem. Soc*. **2004**, *126*, 13639–13641.
(54) Vanderah, D. J.; Valincius, G.; Meuse, C. W. *Langmuir* **2002**, *18*, 4674–4680.
(55) Yang, A.; Galloway, J. A.; Yu, H. *Langmuir* **1999**, *15*, 8405–8411.
(56) Liebman-Vinson, A.; Lander, L. M.; Foster, M. D.; Brittain, M. J.; Vogler, E. A.; Majkrzak, C. F. *Langmuir* **1996**, *12*, 2256–2262.
(57) Sheller, N. D.; Petrash, S.; Foster, M. D. *Langmuir* **1998**, *14*, 4535–4544.
(58) Petrash, S.; Sheller, B.; Dando, W.; Foster, M. D. *Langmuir* **1997**, *13*, 1881–1883.
(59) Choi, E.; Foster, M. D. *Langmuir* **2002**, *18*, 557–561.
(60) Rixman, M.; Dean, D.; Macias, C.; Ortiz, C. *Langmuir* **2003**, *19*, 6202–6218.

Table 2. Coefficients in the Least-Squared Fit to a General Exponential Decay Function (eq 3) [$f_{decay}(t) = f_{60} + a\,e^{-kt}$] for the Data Displayed in Figure 8[a]

sample	f_{60}	a	k (min^{-1})	f_0
solution-HDX-BSA	0.72 ± 0.01	0.06 ± 0.01	0.042 ± 0.040	0.22 ± 0.02
gold-surface-adsorbed-HDX-BSA	0.55 ± 0.01	0.22 ± 0.02	0.102 ± 0.028	0.23 ± 0.03
PS-surface-adsorbed-HDX-BSA	0.34 ± 0.02	0.37 ± 0.03	0.053 ± 0.007	0.28 ± 0.04
PDLLA-surface-adsorbed-HDX-BSA	0.27 ± 0.01	0.43 ± 0.01	0.068 ± 0.005	0.30 ± 0.02

[a] f_0 is the fraction of amide groups that undergo HDX too quickly to be measured by this experiment and is calculated via eq 4. The error bars are derived from using the experimental SD of the mean to weight the significance of each data point in the fitting procedure.

each of the three surfaces and, therefore, imply that the adhesive forces are different in each case.

One possible explanation for this apparent disagreement is that HDX can measure structural changes in the protein caused by a second-order, nonhydrophobic protein/surface interaction (such as hydrogen bonding) that is not sensitively measured via HRFS. However, it is also possible that differences in PS-surface-adsorbed-HDX-BSA and PDLLA-surface-adsorbed-HDX-BSA relate to materials properties that are invariant for Rixman's SAMs (e.g., mechanical properties). Indeed, the behavior of the elastic moduli of PDLLA and PS in $\leq$10.0 nm thick films is expected to be quite different.[61,62]

The BSA unfolding upon adsorption to PDLLA (Figure 8 and Table 2) may also be influenced by changes in the polymer's properties from contact with water. Unlike PS, PDLLA is known to swell and degrade upon hydration.[63−65] In fact, this effect has been shown to increase protein adsorption enough to cause quantitative changes in cellular response.[66,67] We do indeed see evidence of water wetting our PDLLA films, and there is a decrease in measured air−water contact angle of approximately 5° [i.e., from (78 ± 2)° to (74 ± 2)°] after 3 days. However, AFM measurements showed no change in the rms roughness after 3 days of exposure to solvent.

Given the small changes after 3 days, it is no surprise that AFM and contact angle measurements after a 2 h exposure showed no significant swelling changes. These results make it unlikely that surface hydration induced changes are the cause of the difference in f which becomes significant within the first 10 min of exposure, far too fast to be caused by swelling. In addition, differences in f in Figure 8 caused by swelling would be expected to continue to increase throughout the entire experiment. However, our results show a nearly constant difference in f magnitude from 20 to 60 min between the PS and PDLLA surfaces.

It is also possible that surface heterogeneity shields surface-adsorbed amide groups from deuteration, as a rough surface could surround the amides and prevent access by D_2O. In addition, direct contact with the polymer surface could contribute to the observed difference in f for PS-surface-adsorbed-HDX-BSA and PDLLA-surface-adsorbed-HDX-BSA. These shielding effects would depend on the degree of spreading of the protein after adsorption, and there is evidence that the degree of spreading is related to surface chemical properties. In fact, it has been reported that spreading of albumin on very hydrophobic surfaces such as PS can be so severe as to cause a reduction in the mass of the adsorbed layer through surface saturation.[48,49] If PS-surface-adsorbed-HDX-BSA did undergo severe spreading, it would account for the relatively poor quality of the exponential fit (Figure 8 and Table 2) that assumes a single rate-limiting mechanism for HDX. However, the similar secondary structures of the proteins on the polymers would seem to rule out a severe spreading mechanism for one and not the other.

If protein on both polymers is severely spread, then an important step in detailing the mechanism of the protein denaturation by the polymer surfaces is to independently determine changes in protein tertiary structure from changes in secondary protein structure. Our protocol successfully classifies the surface denaturation by the gold surface and in drying from solution as only altering tertiary structure. This tertiary structure denaturation is also present on the two polymer surfaces. However, both polymer surfaces disrupt the BSA's secondary structure. Once the BSA's secondary structure is disrupted and the protein is on the surface, more specific protein/polymer interactions (H-bonding, charge, etc.) become more important and cause greater tertiary structure changes on the PDLLA surface compared to PS.

Conclusions

Classical FTIR curve fitting analysis of the amide I bands revealed BSA adsorbed on PS and PDLLA surfaces has similar secondary structures, but different secondary structures from BSA adsorbed on gold or dried on gold from solution. To compare the protein's tertiary structures on the two polymers, we developed a FTIR-based assay for quantifying the extent of protein denaturation on surfaces via HDX. Our results show that 1 h HDX experiments are sufficient to distinguish between the structure of BSA in solution and in monolayers adsorbed to gold, PS, and PDLLA surfaces. The amount of HDX was greatest for BSA adsorbed to the surface of PDLLA and least in the case of BSA adsorbed to gold, which indicates the greatest and least degree of unfolding, respectively. These results show effects of surface interactions on structure that could not be predicted by hydrophobicity considerations alone. Efforts are currently underway to use the technique introduced in this work to measure relative changes in adsorbed conformation of a variety of proteins, including fibronectin and trypsin, in contact with various polymer surfaces in the context of biomedical materials development.

Acknowledgment. Funding for J.R.S. was provided by a National Academy of Sciences/National Research Council Postdoctoral Fellowship.

(61) Simon, C. G.Jr; Eidelman, N.; Deng, Y.; Washburn, N. R. *Macromol. Rapid Commun.* **2004**, *25*, 2003–2007.
(62) Stafford, C. M.; Harrison, C.; Beers, K. L.; Karim, A.; Amis, E. J.; Vanlandingham, M. R. *Nat. Mater.* **2004**, *3*, 545–550.
(63) Tsuji, H. *Polymer* **2002**, *43*, 1789–1796.
(64) St. Pierre, T.; Chiellini, E. *J. Bioact. Compat. Polym.* **1986**, *1*, 467–497.
(65) Andreopoulos, A. G. E. H.; Doxastakis, M. *J. Mater. Sci. Mater. Med.* **1999**, *10*, 29–33.
(66) Chen, R. I.; Gallant, N. D.; Smith, J. R.; Kipper, M. J.; Simon, C. G. *J. Mater. Sci.: Mater. Med.* **2008**, *19*, 1759–1766.
(67) Safinia, L.; Blaker, J. J.; Maquet, V.; Boccanccini, A. R.; Mantalaris, A.; Bismark, A. *e-Polym.* **2005**, *10*, 1618–7229.